

FAST OPTICAL PYROMETRY

Ared Cezairliyan
Thermophysics Division
National Bureau of Standards
Gaithersburg, Maryland 20899

Abstract

Design and operation of accurate millisecond and microsecond resolution optical pyrometers developed at the National Bureau of Standards during the last two decades are described. Results of tests are presented and estimates of uncertainties in temperature measurements are given. Calibration methods are discussed and examples of applications of fast pyrometry are given. Ongoing research in developing fast multiwavelength and spatial scanning pyrometers are summarized.

1. Introduction

Increasing interest in high-speed studies of high-temperature phenomena and the utilization of dynamic techniques for the measurement of properties of substances at high temperatures has necessitated the development of temperature measurement methods having high time resolution. The definite advantages of noncontact methods in high temperature measurements suggest the selection of optical methods in developing fast high temperature measuring systems.

Various optical methods developed in the past for fast pyrometry are reviewed in the literature [1,2]. Almost all the developments prior to 1970 have been of an exploratory nature. During the last two decades, advances in the field of electronics in general and in fast digital data acquisition systems in particular, coupled with interest in studies of high temperature phenomena, enabled the recent developments of accurate fast pyrometry.

In the present paper, pioneering developments of accurate fast pyrometry at the National Bureau of Standards (NBS) during the last two decades are presented. A summary of the areas of developments and ongoing research on fast pyrometry at NBS is given in Table 1.

Table 1. Fast Pyrometry at NBS

Wavelength Target (μm)	<u>One</u> (0.65)	<u>Two</u> (0.65, 0.9)	<u>Six</u> (0.5, 0.6, 0.65, 0.7, 0.8, 0.9)
Single	Millisecond Resolution	Microsecond Resolution	Millisecond Resolution
Multiple (1024)	Millisecond Resolution		

2. Millisecond-Resolution Pyrometer

The first accurate millisecond-resolution pyrometer was developed by Foley [3] in connection with research on the measurement of high temperature properties of solids by dynamic techniques. The dynamic techniques consist essentially of rapid resistive self-heating of the specimen by the passage of an electric current pulse through it and, with millisecond resolution, measuring the pertinent experimental quantities, such as current through the specimen, potential across the specimen and the specimen temperature. Accurate data on selected thermophysical properties (heat capacity, electrical resistivity, hemispherical total emittance, melting temperature, thermal expansion, temperature and energy of solid-solid phase transformations) were obtained by these techniques up to the melting temperature of refractory solids, primarily metals. A summary of the results is given in the literature [4].

2.1. Salient Features

The salient features of the millisecond-resolution pyrometer [3] are:

1. The pyrometer operates near 0.65 μm . The detector (photomultiplier) is alternately exposed to radiation from the unknown source and to radiation from a reference source. This scheme eliminates errors caused by detector instability and/or drift.
2. The exposure to each source is of the same duration (0.2 ms) and the exposures are uniformly spaced in time.
3. The same detector and associated electronics are used to evaluate every exposure, whether to the unknown or to the reference.
4. Each unknown is evaluated with respect to a member of a "staircase" of three exposures to a reference. A rotating sectorized attenuator produces the "staircase", in which successive attenuation ratios are roughly equal.

5. The output signals are recorded with a digital data acquisition system which has a full-scale resolution of about one part in 8000.
6. The pyrometer can measure the temperature of an unknown source every 0.833 ms. (1200 measurements of temperature per second).

2.2. Optical System

A schematic diagram of the optical system of the millisecond-resolution pyrometer is shown in Fig. 1.

The unknown target X is focused by objective O_x onto a circular field stop F_x . The portion which passes the field stop is collimated by lens M_{x1} , and the aperture of the system is fixed by the circular stop A_x . A magnified image of the field stop is formed by M_{x2} , through right angle prism P, in the plane of the rotating shutter disk DS. When the shutter is open, the radiation passes on through interference filter IF to the photomultiplier PC. The pyrometer range may be extended upwards by inserting neutral density filters in the collimated beam between lenses M_{x1} and M_{x2} .

Radiation from the steady reference source R is focused by objective O_r on field stop F_r , is collimated by M_{r1} , and the aperture is limited by A_r . The collimated reference radiation then passes through the rotating attenuator disk DA, mounted on the opposite end of the motor shaft from the shutter disk DS. The image of F_r is focused in the plane of the shutter disk by M_{r2} . The reference radiation falls on the same circular area of the photocathode, when the shutter is open to the reference source, as does the radiation from the unknown source when the shutter is open to the latter.

The two pairs of stops (F_x - F_r and A_x - A_r) and the two pairs of lenses (M_{x1} - M_{r1} and M_{x2} - M_{r2}) are all as nearly alike as possible. So that the two optical channels are substantially identical, except that the unknown channel contains prism P and the reference channel contains the attenuator disk DA. The differences in the optical channels are accounted for during calibration.

The metal attenuator disk DA has three pairs of sectors around its circumference. One pair of sectors is cut away so that light passes freely. Another pair of sectors is perforated in a pattern of small square holes, so as to transmit somewhat less than 50% of the radiation which falls on the sector. A third pair of sectors is similarly perforated with smaller holes, so as to transmit somewhat less than 25%. The number of holes is made very large, so that any fluctuation in transmission during the rotation of the disk because of the finite number of holes is negligible by comparison with the noise due to the finite number of photons in each sample. The effective transmittance of the attenuator is determined experimentally in a calibration procedure, accounting for any diffraction effects which occur. As the disk rotates, the reference illumination thus changes in three steps

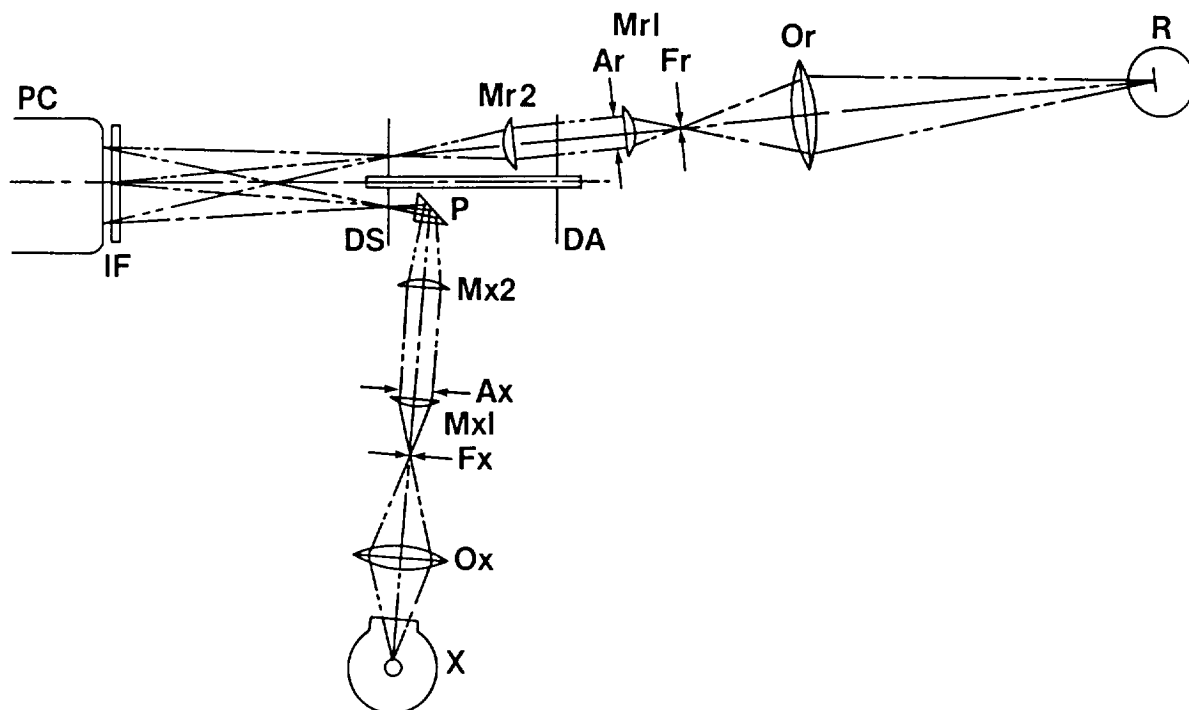


Figure 1. Schematic diagram of the optical system of the millisecond-resolution pyrometer.

during each half-revolution. A film of transparent resin covers the perforated areas to prevent dirt from changing the effective size of the openings.

The shutter disk has six large apertures each subtending 15° at the center of the disk. It and the attenuator disk are rotated at 200 rps by a synchronous motor. The shutter disk opens the reference radiation path for $208\ \mu\text{s}$, then closes for $208\ \mu\text{s}$, then opens the unknown radiation path for $208\ \mu\text{s}$, closes for $208\ \mu\text{s}$, and then opens the reference path again. The reference pulses form two "staircases" per revolution of the sampling motor; the unknown pulses are interlaced with the reference pulses. The shutter disk also has a circle of timing apertures, which is used to generate photoelectrically the pulses to control the electronic system.

The optical system was designed to view a target circle 0.2 mm in diameter on the unknown from a distance of 10 cm. The nominal wavelength passed by the interference filter is $0.65\ \mu\text{m}$, and the nominal bandwidth of the filter is $0.01\ \mu\text{m}$.

2.3. Electronic System

The radiation detector is an end-on type photomultiplier with S-20 cathode, mounted so as to reduce microphonism and to minimize the influence of magnetic fields. The photomultiplier anode is connected directly to the summing junction of an operational amplifier, which in turn feeds an integrator. The integrating capacitor is shunted by a silicon diode, connected so that it is reverse biased when photocurrent flows. $2 \times 10^{-8} \text{ C}$ from the photomultiplier anode will charge the integrator to its maximum value of 10 V.

A synchronization and control system accepts the timing signals from the pyrometer and separates them into two pulse streams, one containing the synchronizing pulses which occur per revolution of the sampling motor, and the other containing 12 start pulses per revolution. The start pulses trigger the digitization of the integrator voltage, and each generates a delayed pulse to reset the integrator after an appropriate time. The synchronization pulse, once per revolution, is used to store the data in orderly fashion for delayed processing by a computer.

The signals from the pyrometer electronics are recorded with a digital data acquisition system which has a full-scale resolution of about one part in 8000 (2^{13})

2.4. Calibration

A calibration is first made under steady-state conditions to determine parameters inherent to the pyrometer, by comparing the radiation of the standard lamp to that of an equivalent reference lamp. These parameters are then used in the determination to compare the reference lamp radiation with the specimen radiation under conditions of rapidly changing temperature. The Wien radiation equation, modified for use with this pyrometer, serves as the transfer mechanism. The steady-state calibrations utilizing the gas-filled tungsten-strip lamps are for temperatures up to about 2500 K, the limit of reliable operation for such lamps. For measurements at higher temperatures, calibrated optical attenuators are placed in the path of the radiation from the specimen.

2.5. Performance

The sources and magnitudes of uncertainties in temperature measurements with the millisecond-resolution pyrometer are discussed in detail in the literature [5] and are summarized in Table 2. It may be concluded that the uncertainty in temperature measurements is approximately 3 K at 2000 K and 6 K at 3000 K. It should be noted that factors such as departure from ideal blackbody conditions and temperature nonuniformity of the specimen are not included in the above figures. The resolution or sensitivity of the pyrometer defined as the standard deviation (of an individual point) from the mean of a large number of temperature measurements is 2 K at 1200 K, 0.6 K at 1500 K and about 0.3 K at 2000 K.

Table 2. Estimated Uncertainties in Temperature Measurements with the Millisecond-Resolution Pyrometer [3,5].

Source of Error	Uncertainty, K	
	at 2000 K	at 3000 K
Standard Lamp Calibration	2	4
Instability of Standard Lamp	0.5	1
Radiation Source Alignment	1	2
Pyrometer Calibration Instability	1	2
Scattered Light Correction	0.5	1
Attenuator Calibration	1	2
Window Effects	1	2
Total Uncertainty in Temperature*	3	6

*Root sum square of above items rounded to the higher single significant figure.

2.6. Example of Operation

The millisecond-resolution pyrometer has been successfully used for the determination of selected thermophysical properties of solids at high temperatures utilizing a pulse heating technique [4]. As an example, measurement of the melting temperature of niobium [6] is shown in Fig. 2. The specimen was a tube of the following nominal dimensions: length, 102 mm; outside diameter, 6.3 mm; thickness, 0.5 mm. A small rectangular hole (0.5 x 1 mm) fabricated in the wall at the middle of the specimen approximated blackbody conditions for temperature measurements.

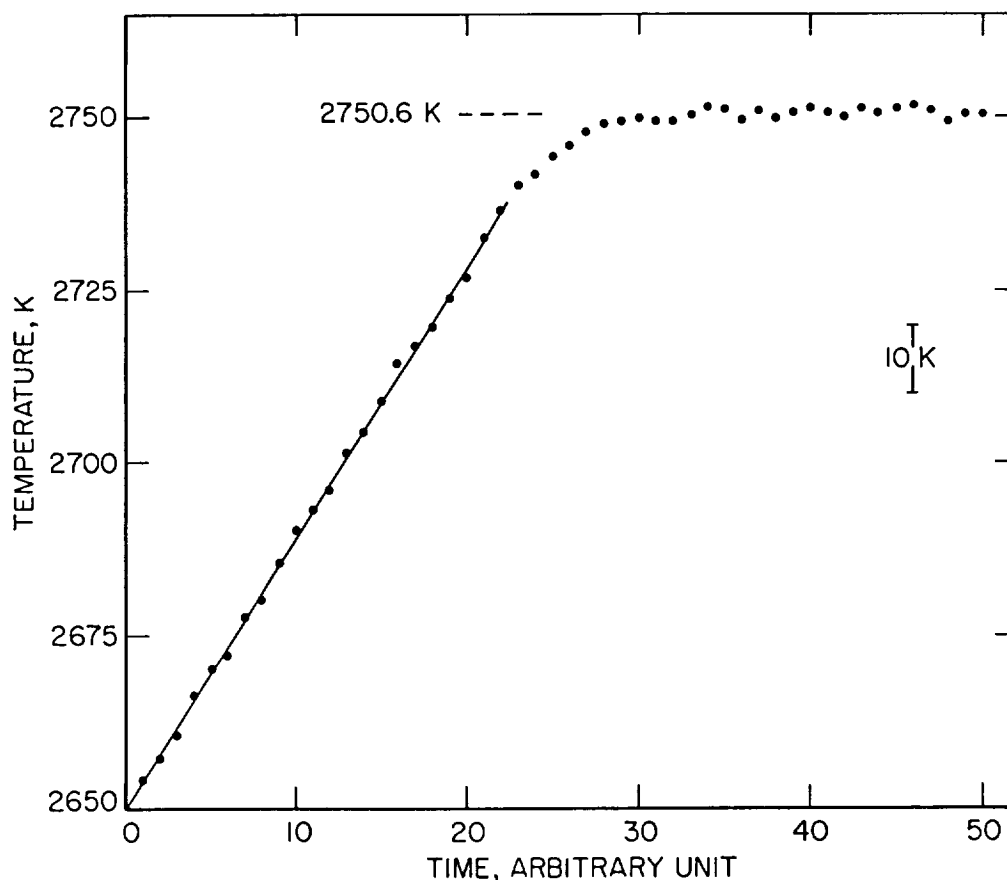


Figure 2. Temperature of a heating niobium specimen as a function of time near and at the melting point measured with the millisecond-resolution pyrometer. The plateau in temperature indicates melting of niobium (1 time unit = 0.833 ms).

3. Microsecond-Resolution Pyrometer

An accurate microsecond-resolution pyrometer was developed at the National Bureau of Standards by Foley et al. [7] in connection with research to extend the measurement of properties of substances far beyond their melting temperatures and up to 6000 K. The unfavorable conditions associated with very high temperatures, such as increases in heat loss, chemical reactions, evaporation, etc., have brought forward an entirely new set of experimental problems, which necessitated the development of ultra-fast measurement techniques. The microsecond-resolution dynamic technique, incorporates the pyrometer developed by Foley et al. [7], is described in the literature [8]. Application of this technique to measurements of heat of fusion and properties of liquid metals at high temperatures is presented elsewhere [9].

3.1. Salient Features

The salient features of the microsecond-resolution pyrometer [7] are:

1. The pyrometer is sufficiently fast and precise to justify the recording of its signals by a digital data acquisition system at regular intervals as short as $1.5 \mu\text{s}$ with a resolution of 0.1 percent.
2. The pyrometer measures radiance temperatures in two narrow spectral regions, $0.65 \mu\text{m}$ and $0.9 \mu\text{m}$.
3. In order to minimize the effect of electromagnetic interference, the electronics of the pyrometer are entirely outside the shielding of the room in which dynamic experiments are conducted. Radiation selected by the optics in each of the two spectral regions is transmitted by fiber optic cables through the shielding walls to the detectors and their associated electronic circuits.
4. The pyrometer uses high-speed automatic gain switching of linear amplifiers to achieve high stability, high resolution and wide temperature range.

3.2. Optical System

Figure 3 shows the optical arrangement of the pyrometer. An objective lens O forms two images of the target T at the field stops S1 and S2 by means of the beam splitter B. Filter F1 passes radiation near $0.65 \mu\text{m}$ to S2; each filter has a bandwidth of $0.03 \mu\text{m}$. This design permits the two field stops to be focussed independently to minimize the effects of chromatic aberration. The field stops are 0.5 mm diameter and the magnification is unity, so the target is the same size. The radiation passing through each field stop falls on the end of one of two fiber optic cables, C1 or C2, for transmission to silicon diode photodetectors. The stops are so close to the ends of the cables that the stops, and not the cables, define the target areas. A mirror M can be swung into the path between objective lens and beam splitter to form the image of the target at a reticle R. The experimenter aims and focuses the instrument by viewing the reticle and target image through a microscope.

3.3. Electronic System

The silicon diode detectors used were specially chosen for good stability and linearity. The photocurrents are converted to voltages and amplified by a series of operational amplifiers. The analog output of each amplifier channel is applied to a 10-bit high-speed analog-to-digital converter (ADC). Other ADCs digitize voltages proportional to the heating current and to the voltage drop in the specimen. Another signal which gives the ranges of the pyrometer channels is also digitized. Various digitizing intervals from 1.5 to $512 \mu\text{s}$ may be chosen. 1024 10-bit words of digital data may be stored from each of five data channels in a semiconductor memory.

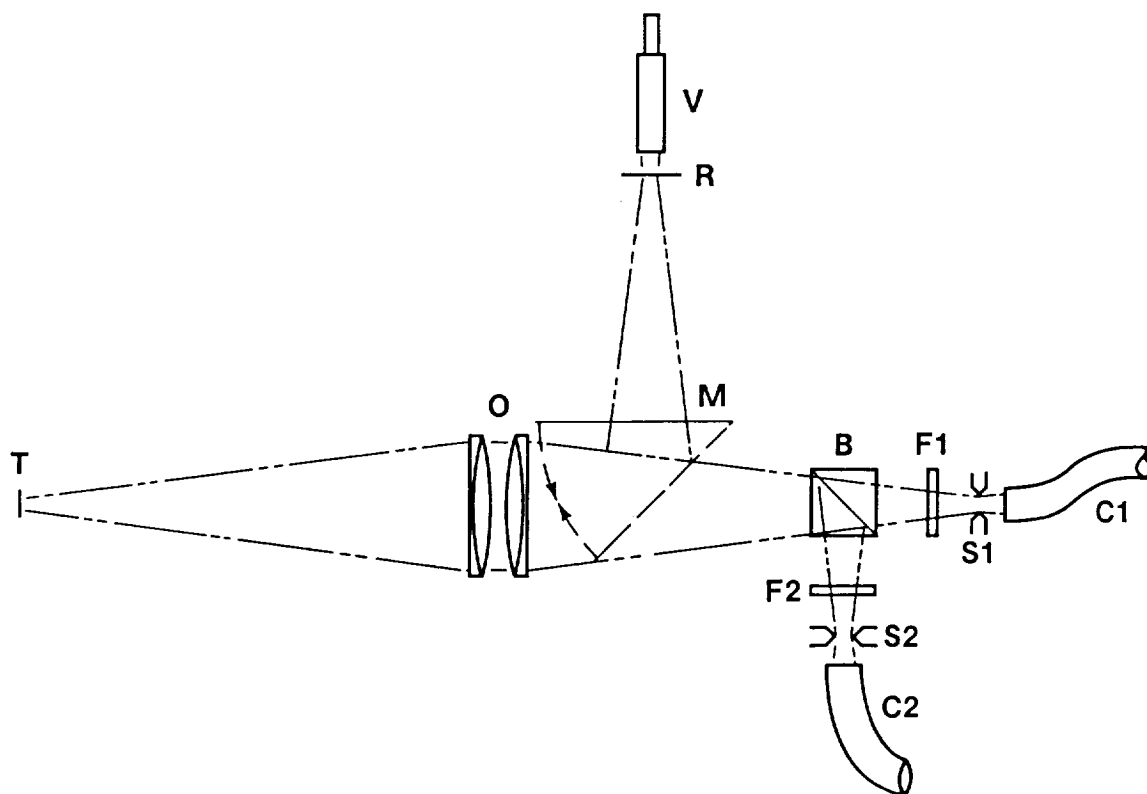


Figure 3. Schematic diagram of the optical system of the two-color microsecond-resolution pyrometer.

The digital recording system limits the temperature resolution of the pyrometer. If the photocurrents were amplified at fixed gain before digitization, there would be adequate resolution, as compared with the precision and accuracy, at the upper end of any selected temperature range, but not enough at lower temperatures, even when the specimen emitted sufficient energy for accurate pyrometry. Logarithmic amplifiers theoretically would give wide range and acceptably uniform resolution. In tests, however, several high-speed logarithmic amplifiers drifted so rapidly that the results of steady state calibrations could not be used to interpret the data from experiments which were performed only a few minutes before or after the calibration.

The pyrometer uses linear amplifiers with high-speed automatic gain switching. The output of each channel is switched through as many as three overlapping ranges. This procedure uses fast, stable components, and results in a response which approximates the logarithm of the input. Changes in amplifier gain are completely negligible. The precision is limited by short term zero drift which on the most sensitive (lowest temperature) range is less than 0.05% over an hour. The useful range of the amplifier extends over more than 3 decades of photo-current. Figure 4 is a block diagram of the analog electronics of each channel.

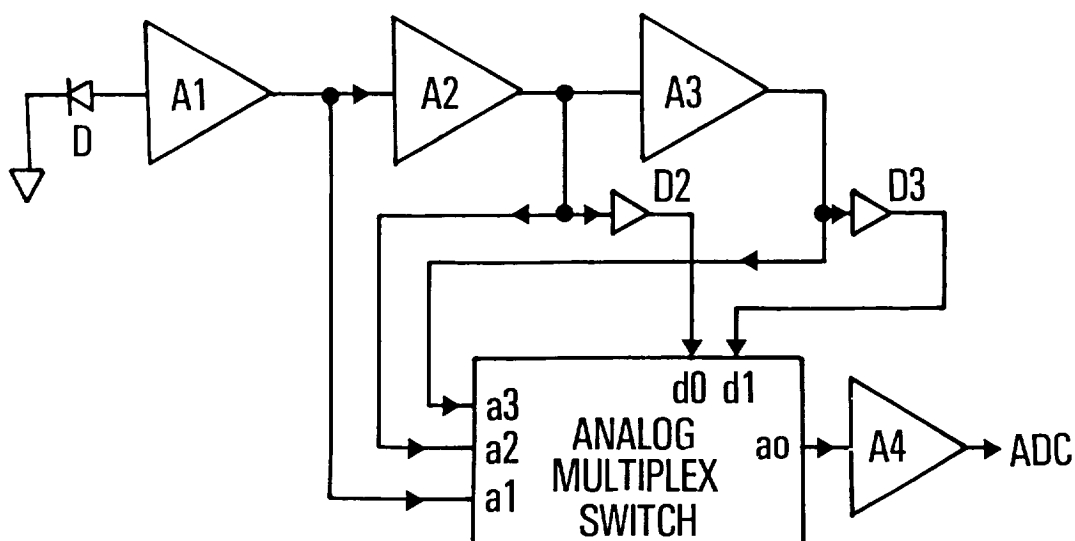


Figure 4. Block diagram of the analog electronics of each channel of the two-color microsecond-resolution pyrometer.

The output voltages of amplifiers A2 and A3 are compared with an 8 volt reference. If an amplifier output voltage exceeds the reference, that stage is switched out of the amplifier chain to reduce the gain; if it falls below the reference, the stage is switched in again, increasing the gain. The transresistance of amplifier A1 in each channel is 30,000 V/A and the gain of each amplifier A2 and A3 is 11. Switching from low to midrange occurs when the photocurrent rises above 2.2 μA , and from midrange to high range at a photocurrent of 24 μA . The maximum output on the high temperature range is reached at a photocurrent of 0.37 mA. The corresponding radiance temperature ranges are:

Range	0.65 μm Channel	0.9 μm Channel
Low	1960 - 2520 K	1545 - 2030 K
Mid	2500 - 3460 K	2015 - 2920 K
High	3430 - 5700 K	2885 - 5500 K

3.4. Calibration

A gas-filled tungsten-strip lamp was calibrated by the Radiometric Physics Division of the National Bureau of Standards. The calibrations covered the range 1873-2573 K at 0.65 μm and the range 1800-2425 K at 0.9 μm . The pyrometer was used to record the radiance from the calibrated lamp at eight values of filament current identical with those specified on

the certificate of calibration. Each measure of response, together with an appropriate measure of dark response was used to determine the calibration constant. These values were used in turn to calculate a weighted mean for each channel, using the measured response as the weighting factor. The weighted means for the calibration constant were then used to attribute spectral radiance temperatures to the lamp. The differences between the calibration values and the measurements lay between 0.1 to 2.0 K for the 0.65 μm channel and between 0.1 and 0.6 K for the 0.9 μm channel for each of eight spectral radiances.

3.5. Performance

The sources and magnitudes of uncertainties in temperature measurements with the microsecond-resolution pyrometer are discussed in detail in the literature [7] and are summarized in Table 3. The table gives the estimate of uncertainty in spectral radiance as a percentage of the radiance for the temperature and channel involved. The square root of the sum of the squares of the various individual uncertainties is taken to be the probable uncertainty of spectral radiance for the pyrometric system as a whole, and this number is converted to an uncertainty in temperature. To summarize the uncertainty in temperature measurements, data are given for the low and high end of each range in each channel. Since the temperature ranges of the two channels are different, twelve estimates are given for seven different temperatures, six of the estimates referring to each of the two channels.

3.6. Example of Operation

To demonstrate the measurement of temperature under dynamic conditions, a niobium rod, 25 mm long and 1.6 mm diameter, was heated rapidly with the use of the capacitor discharge system described elsewhere [8]. The results of the radiance temperature measurement by the pyrometer are shown in Fig. 5. The plateaus in the temperature plot show the melting of the niobium. It can be seen that the pyrometer followed the entire melting, and continued to show reasonable values of spectral radiance temperature for several hundred degrees into the liquid phase.

The entire time, from room temperature to near 3500 K, was only 100 μs . Melting of the niobium took place in about 15 μs . The average radiance temperatures measured at the melting point of niobium are 2431 K at 0.65 μm and 2250 K at 0.9 μm . The difference in the radiance temperatures at the two wavelengths is due to the difference in normal spectral emittance of the metal at the two wavelengths.

4. Multiwavelength Pyrometer

Recently, a fast multiwavelength (six-channel) pyrometer was designed and constructed at the National Bureau of Standards by Foley et al. [10]. The pyrometer is intended to be used for: (1) simultaneous determination of the radiance temperature of metals at their melting points at several wavelengths as possible temperature reference points and (2) exploration of the possibility of improving the determination of true temperature from measurement of the spectral radiance temperature of incandescent objects in a number of spectral bands.

Table 3. Estimated Radiance Uncertainties* of Two-Color Microsecond Pyrometer

0.65 μm Channel

Temperature, K	Low Range		Mid Range		High Range	
	2000	2500	2500	3450	3450	5500
Secondary Standard, %	0.7	1.0	1.0	1.0	1.0	1.0
Acceptance Angle, %	0.4	0.4	0.4	0.4	0.4	0.4
Effective Wavelength, %	0	0	0	0	0	0
Amplifier Drift, %	0.01	0.02	0.01	0.02	0.01	0.02
Nonlinearity, %	0	0	0	0.2	0.2	2.0
Total Noise, %	2.5	0.5	0.2	0	0	0
Quantization, %	1.0	0.2	1.0	0.2	1.0	0.2
Transfer, %	2.7	0.5	0.5	0.5	0.5	0.5
Root Mean Square, %**	3.9	1.3	1.6	1.2	1.6	2.3
Uncertainty, K***	7.1	3.7	4.4	6.2	9.9	32

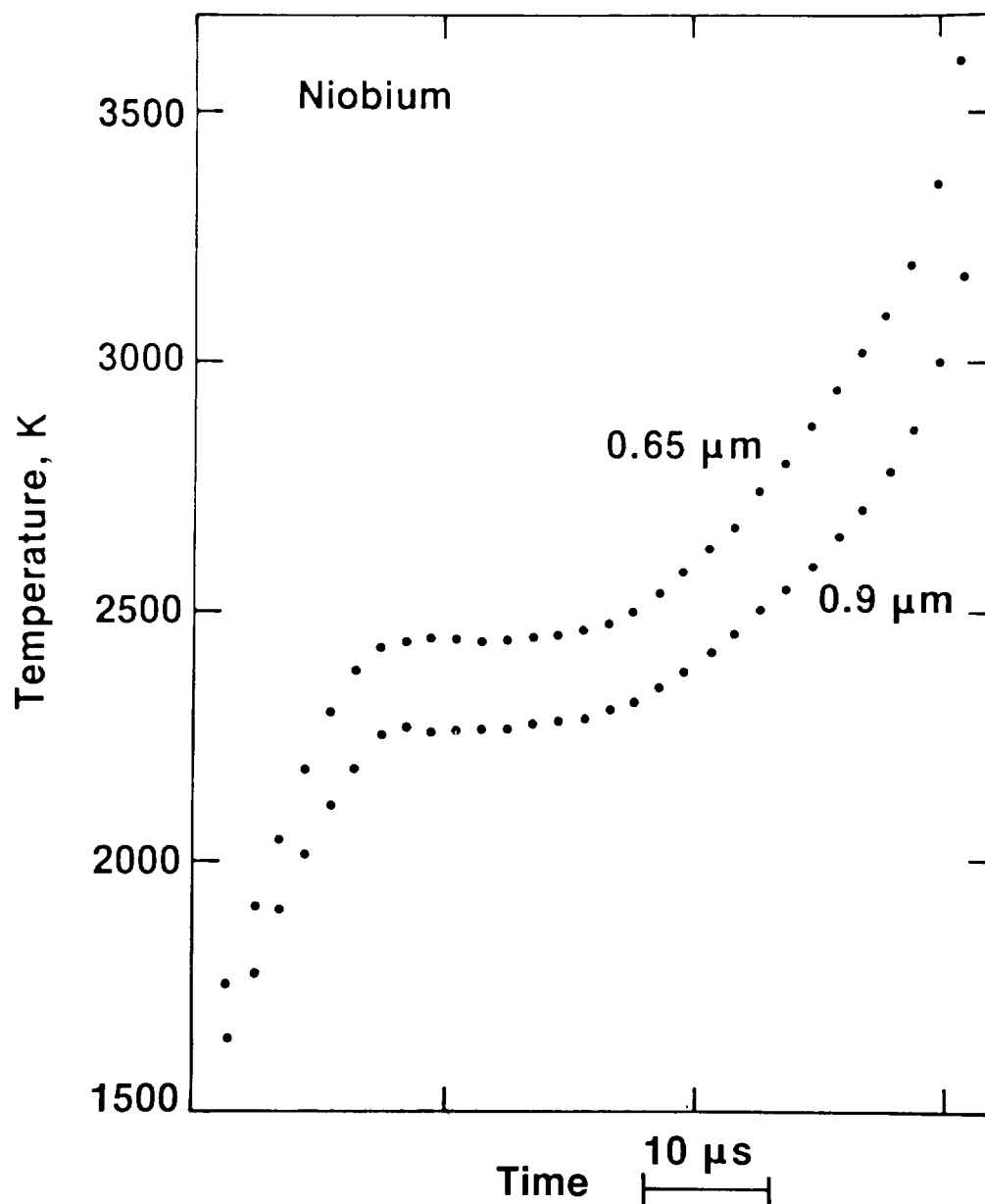
0.9 μm Channel

Temperature, K	Low Range		Mid Range		High Range	
	1550	2025	2025	2900	2900	5500
Secondary Standard, %	1.0	1.1	1.1	1.1	1.1	1.1
Acceptance Angle, %	0.4	0.4	0.4	0.4	0.4	0.4
Effective Wavelength, %	0.1	0.1	0.1	0.1	0.1	0.1
Amplifier Drift, %	0.01	0.02	0.01	0.02	0.01	0.02
Nonlinearity, %	0	0	0	0.2	0.2	2.0
Total Noise, %	2.5	0.5	0.2	0	0	0
Quantization, %	1.0	0.2	1.0	0.2	1.0	0.2
Transfer, %	2.7	0.5	0.5	0.5	0.5	0.5
Root Mean Square, %**	4.0	1.4	1.6	1.3	1.6	2.4
Uncertainty K***	6.0	3.6	4.2	6.9	8.6	19

* Estimates of uncertainties are expressed as a percentage of radiance for a given temperature and channel.

** Root mean square of the listed individual uncertainties.

*** Root mean square uncertainty expressed in temperature.



4.1. Salient Features

The salient features of the multiwavelength pyrometer [10] are:

1. The pyrometer measures spectral radiance temperature above 1500 K.
2. The pyrometer has six channels. Five of the channels have a spectral bandwidth of about $0.1\ \mu\text{m}$, centered near 0.5, 0.6, 0.7, 0.8, and $0.9\ \mu\text{m}$. The sixth channel has a bandwidth of $0.03\ \mu\text{m}$ centered at $0.65\ \mu\text{m}$.
3. The pyrometer can make a set of six measurements every 0.1 ms.
4. The pyrometer has two modes of operation. In the first mode, signals from all the channels are digitized and recorded simultaneously. In the second mode, the channels are multiplexed and thus signal from one channel is recorded at a given time.

4.2. Optical System

An objective lens of unity magnification, made up of a pair of identical achromats, focusses the radiation from the target on a single field stop, defining a circular target area of 0.5 mm in diameter. A mirror can be swung into the path between the objective lens and the field stop to form an image of the target on a reticle. The optical path length from objective to reticle is adjusted to equal that from objective to field stop. For aiming and focussing, a microscope is used to view a 0.5 mm circle drawn on the reticle.

The light passing the field stop illuminates a fiber optic bundle. The latter is divided, nominally at random, into six separate bundles which illuminate six interference filters and silicon diode detectors. The ends of the fiber bundles are placed as close as possible to the detectors in an effort to maximize efficiency, but the fibers cannot be allowed to come too close to the filters, nor the filters to the detector windows, lest optical interference effects distort the spectral response.

4.3. Electronic System

High-stability amplifiers convert the photocurrents from the diodes to proportionate voltages, which are switched sequentially through a semi-conductor multiplexor to feed a line-driver amplifier. Each conversion amplifier has three different manually selected feedback resistors to give "low", "medium" and "high" temperature ranges. The low temperature range feedback resistors were originally intended to give an output voltage of 0.4 V from each of the amplifiers when the spectral radiance temperature was 2000 K. This called for the resistors to differ from one another by as much as sixteen times because of the variation in spectral radiance of the source and in sensitivity of the detectors over the spectral range of the pyrometer channels. The medium temperature range resistors were intended to give 0.4 V at 2700 K and the high temperature range resistors to give 0.4 V at

4500 K. Experimental results with the completed pyrometer caused us to alter the values of some of the low range resistors. To maximize stability the largest resistors are 7 megohms.

4.4. Calibration

The channel centered near $0.65\ \mu\text{m}$ with $0.03\ \mu\text{m}$ bandwidth, was calibrated by averaging 100 successive values of output voltage when viewing the filament of a calibrated gas-filled tungsten strip lamp, and subtracting the mean of 100 successive values of output voltage when dark. The calibration was made at or near each of six or seven values of lamp current specified on the certificate of calibration. The calibration constant is the output voltage divided by the value of the integral, taken over the spectral band, of the pyrometer transmission times the window transmission times the Planck function at the radiance temperature given on the certificate. It should, of course, be the same for every temperature, but in fact noise and other errors give different values for each of the lamp currents. The calibration procedure is considered satisfactory if the variation among the values for the constant is small and is not systematic. For later determination of an unknown temperature we use the mean of the calibration constants, weighted by the pyrometer voltage. This gives greater weight to the higher temperature points where noise has less effect on the result.

The calibration of the $0.65\ \mu\text{m}$ channel was transferred to the other channels in a dynamic experiment. The source was a graphite cylinder 6.4 mm diameter and 100 mm long, clamped to have an effective length of 45 mm., with a rectangular hole 1.6 mm high and 1 mm near the center of the length of the 1 mm thick wall. This tube was heated in argon by a pulse of direct current from large lead acid storage cells. The pyrometer viewed the radiation emitted from the hole at an angle of about 10 degrees from radial during the heating period. The blackbody quality of this specimen is calculated to be 0.994. The recording of the pyrometer output was begun before the heating current pulse was turned on, so that the dark response of all the channels was recorded and an average calculated for subtraction from the values recorded from the hot specimen. At intervals during the heating pulse, the measured output from the calibrated $0.65\ \mu\text{m}$ channel was interpreted to find the radiance temperature at that wavelength. This was assumed to be the true temperature, and this "true" temperature was used with the data from all six channels to determine, by the same method of numerical integration as described above in connection with the calibration using the tungsten strip lamp, a calibration constant for each channel. A weighted average of these calibration constants was then calculated for each channel.

4.5. Performance

The multiwavelength pyrometer has just become operational, thus no significant amount of data have been obtained to assess its operation, the uncertainty of radiance temperature measurements, and its ability to yield true temperature from measured radiance temperatures. At present, work is in progress to test the pyrometer.

4.6. Example of operation

Preliminary measurements of the radiance temperature of niobium at its melting point were performed with the multiwavelength pyrometer. A total of ten experiments were conducted where niobium specimens were melted by utilizing a transient resistive self-heating technique in short times (less than 1 s). Measured radiance temperatures at a given wavelength were all within ± 2 K of the average for that wavelength. The average radiance temperatures as a function of wavelength at the melting point of niobium are shown in Fig. 6.

5. Spatial Scanning Pyrometer

Recently, a fast spatial scanning pyrometer was designed at the National Bureau of Standards. Construction of this pyrometer has begun. The scanning pyrometer is a monochromatic optical pyrometer using a self-scanning linear array of silicon photodiodes as a detector. It will rapidly measure the spectral radiance temperature at 1024 points along a straight line in the target field. This will permit measurements of temperature gradients in a rapidly heating specimen providing data for both diagnostic purposes and determining thermal diffusivity which will be a novel approach suitable for measurements at very high temperatures.

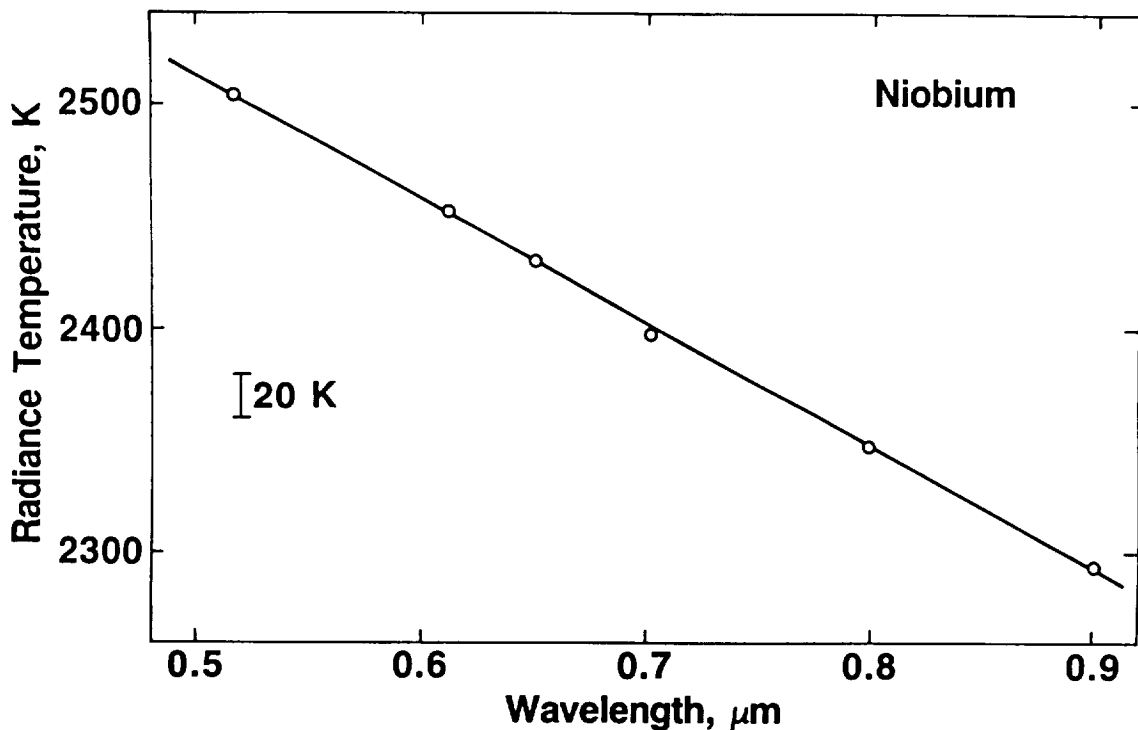


Figure 6. Radiance temperature of niobium at its melting point as a function of wavelength measured with the millisecond-resolution multiwavelength pyrometer.

5.1. Salient Features

The salient features of the spatial scanning pyrometer are:

1. The pyrometer will measure spectral radiance temperature at 1024 points along a straight line (25 mm long).
2. A complete cycle of measurements (1024 points) will be performed in about 1 ms.
3. The radiance temperature measurements will be performed at $0.65\ \mu\text{m}$ (bandwidth: $0.03\ \mu\text{m}$).

5.2. Optical System

The basic optical design is a further modification of that used in the multiwavelength pyrometer. The design provides an unobstructed path slightly smaller than 50 mm in diameter from the back of the objective lens to the pyrometer faceplate. The objective lenses are made from a pair of standard achromats 52 mm in diameter, and 200 mm nominal focal length. The interference filter to establish the effective wavelength of the pyrometer is mounted as close as possible to the diode array. The peak of the interference filter is at around $0.65\ \mu\text{m}$, and the bandwidth is about $0.03\ \mu\text{m}$. A circular mirror is mounted on a platform hinged near the partition carrying the diode array so that it can swing down and intercept all of the light from the lens and direct it to a focus on a reticle carrying a scale 20 mm long graduated in tenths of a millimeter. A suitable eye-lens gives a reasonably magnified view of the whole scale.

5.3. Electronic System

The self-scanning array contains 1024 diodes with a center-to-center spacing of $25\ \mu\text{m}$ and so is about 25 mm long. Each diode of the array is nominally $15\ \mu\text{m}$ long and $26\ \mu\text{m}$ wide. It is presently planned to use the array with a lens system having unity magnification so that the target region will be about 25 mm.

Each photodiode of the array has associated with it a shunt capacitance. One end of the diode-capacitor pair is connected to the positive end of the power supply and the other end is connected through an FET switch to a common video recharge line. The switch is closed briefly by a "start" pulse passing down a 1024 stage shift register being connected to each of the 1024 switches associated with the photodiodes. When the photodiode switch first closes another FET switch closes to connect the common video recharge line to the video buffer amplifier, which stores the voltage present on the recharge line. The video buffer FET is then opened and a recharge FET switch is closed to the negative power supply to recharge the photodiode capacitor. The "start" pulse then shifts to the next stage of the shift register, opening the photodiode switch on the preceding diode and closing the switch on the next. When the start pulse passes from the last stage of the shift register it goes to the external circuits as an End-Of-Line (EOL) signal.

The next "start" pulse is applied to the first stage of the shift register after a programmable delay of at least eight clock pulses, to connect the first photodiode and its associated capacitor to the video buffer. The voltage of the recharge line at this time is reduced below its value at the previous recharge time in proportion to the photocurrent flowing in the photodiode since the last start pulse. The voltage difference thus represents the integral of the illumination of the photodiode during the scanning period.

The signal from the buffer is summed with a signal from dummy diodes, to reduce switching noise and compensate for temperature effects, and passed to the motherboard. Here it is subjected to another sample-and-hold operation to clean up more of the switching noise and reestablish the dark level.

It seems that the linear range of the system is primarily fixed by the characteristics of the photodiode part of the array integrated circuit. Even if the photodiode capacitor is fully discharged after one scanning interval, the voltage to which the video recharge line stabilizes during sampling will be reduced by the ratio of the capacitance associated with each photodiode to the capacitance of the common video recharge line, the FET switch to the video buffer and the buffer itself. If this ratio is significantly affected by array temperature, both the sensitivity and saturation level will vary.

5.4. Status

At present, the spatial scanning pyrometer is being constructed. It is anticipated that by the end of 1987, it will be ready for testing.

6. Summary

Accurate fast pyrometers developed at the National Bureau of Standards have demonstrated the possibility of performing dynamic temperature measurements with an uncertainty of 3 K at 2000 K and 6 K at 3000 K with millisecond resolution, and 7 K at 2000 K and about 30 K at 6000 K with microsecond resolution. Recently, construction of a millisecond-resolution six-wavelength pyrometer was completed and its testing has begun. When fully operational, this pyrometer will yield important information on normal spectral emittance of surfaces and on reliability of determining true temperature from spectral radiance temperature measurements. A new millisecond-resolution spatial scanning pyrometer is also designed which will be able to measure temperatures at 1024 points along a straight line in times of the order of 1 ms.

The fast pyrometers have already found applications in measurements of thermophysical properties at high temperatures utilizing millisecond and microsecond resolution dynamic techniques. In the future they will become important measuring and diagnostic instruments in research on time-dependent phenomena at high temperatures and related new fields in materials sciences.

7. References

1. A. Cezairliyan, "Measuring Transient High Temperatures by Optical Pyrometry", in Temperature, Vol. 4, Part 1, H.H. Plumb, ed. (Instrument Society of America, Pittsburgh, 1972) p. 657.
2. A. Cezairliyan, J.F. Babelot, J. Magill, and R.W. Ohse, "Fast Radiation Thermometry", in Theory and Practice of Radiation Thermometry, D.P. DeWitt and G.D. Nutter, eds., in press.
3. G.M. Foley, Rev. Sci. Instrum., 41, 827 (1970).
4. A. Cezairliyan, Int. J. Thermophysics, 5, 177 (1984).
5. A. Cezairliyan, M.S. Morse, H.A. Berman, and C.W. Beckett, J. Res. Nat. Bur. Stand. (U.S.), 74A, 65 (1970).
6. A. Cezairliyan, High Temp.-High Press., 4, 453 (1972).
7. G.M. Foley, M.S. Morse, and A. Cezairliyan, "Two-Color Microsecond Pyrometer for 2000-6000 K" in Temperature, Vol. 5, J.F. Schooley, ed. (Am. Inst. Physics, New York, 1982) p. 447.
8. A. Cezairliyan, M.S. Morse, G.M. Foley, and N.E. Erickson, "Microsecond Resolution Pulse Heating Technique for Thermophysical Measurements at High Temperatures", in Proceedings of the Eighth Symposium on Thermophysical Properties, Vol. 2, J.V. Sengers, ed. (Am. Soc. Mech. Eng., New York, 1982) p. 45.
9. A. Cezairliyan and J.L. McClure, Int. J. Thermophysics, 8, No. 5 (1987), in press.
10. G.M. Foley and A. Cezairliyan, "Millisecond Resolution Multiwavelength Pyrometer", in preparation.